Hypoxic Encephalopathy after Near-Drowning Studied by Quantitative ^{1}H-Magnetic Resonance Spectroscopy

Metabolic Changes and Their Prognostic Value

Roland Kreis,*§ Edgard Arcinue,‡ Thomas Ernst,* Truda K. Shonk,* Ricardo Flores,‡ and Brian D. Ross*

**Huntington Medical Research Institute and ‡Huntington Memorial Hospital, Pasadena, California 91105; and §University of Bern, CH-3010 Bern, Switzerland*

Abstract

Early prediction of outcome after global hypoxia of the brain requires accurate determination of the nature and extent of neurological injury and is cardinal for patient management. Cerebral metabolites of gray and white matter were determined sequentially after near-drowning using quantitative ^{1}H nuclear magnetic resonance spectroscopy (MRS) in 16 children. Significant metabolite abnormalities were demonstrated in all patients compared with their age-matched normal controls. Severity of brain damage was quantified from metabolite concentrations and ratios. Loss of *N*-acetylaspartate, a putative neuronal marker, from gray matter preceded that observed in white matter and was more severe. Total creatine decreased, while lactate and glutamine/glutamate concentrations increased. Changes progressed with time after injury.

A spectroscopic prognosis index distinguished between good outcome ($n = 5$) and poor outcome ($n = 11$) with one false negative (bad outcome after borderline MRS result) and no false positive results (100% specificity). The distinction was made with 90% sensitivity early (after 48 h) and became 100% later (by days 3 and 4). This compared with 50–75% specificity and 70–100% sensitivity based upon single clinical criteria.

MRS performed sequentially in occipital gray matter provides useful objective information which can significantly enhance the ability to establish prognosis after near-drowning. (*J. Clin. Invest.* 1996. 97:1142–1154.) Key words: *N*-acetylaspartate • glutamine • creatine • prognosis • brain

Introduction

The term near-drowning (ND)[1] is applied to patients with cardiac arrest and asphyxia after submersion in water, who are resuscitated and survive beyond 24 h. ND is one of many causes of hypoxic encephalopathy, all of which present problems of prognosis and management in intensive care units (ICU) and in long-term care (1, 2). Acute hypoxic injury to the brain has been studied extensively in laboratory animals (3–6). It principally concerns arrest of electron transport and ATP synthesis leading to a myriad of secondary changes, with the two most detrimental consequences being brain edema and central nervous system cell death. The course of events after hypoxia is not only determined by the direct effects of biochemical dysequilibria (including imbalances of ions and chemical mediators like glutamate or oxygen radicals), but is indirectly influenced by the hypoxic effects on reperfusion (no reflow phenomenon [7]). In victims of ND, global cerebral circulation and O_2 supply are successfully restored, and it is the secondary effects of hypoxic brain injury which are manifested and documented in this magnetic resonance spectroscopy (MRS) study.

After ND, three distinct outcomes are recognized: death, survival with severe neurological impairment (persistent vegetative state, PVS), or recovery to normal neurological function. The majority of patients entering the ICU in a flaccid, comatose state will suffer cerebral death or severe long-term neurologic sequelae. Trials aimed at restoring hypoxic-damaged brain have been largely unsuccessful (8). However, as many as 30% of patients will survive ND neurologically intact (9), but predicting the outcome in individual patients has proven to be difficult. Suggested indicators include: temperature of submersion medium (10), duration of submersion, Glasgow coma score (GCS), rapidity of restoration of heart beat, state of pupils, minimum blood pH, intracranial pressure, reduction in regional blood flow, EEG, and blood glucose (11, 12). None of these factors, either individually or in combination, have been universally successful. Recently, neurological status after 24 h (13) or reduction in cerebral arterio-venous oxygen difference and cerebral oxygen consumption have shown some utility in distinguishing good from bad outcome (14). Because of the imprecision of such clinical measurements, there is an urgent need for new objective prognostic tests. Ideally, they should also define the nature and extent of secondary hypoxic injury to identify new therapeutic opportunities. Because ND is so reproducibly a cause of global hypoxic encephalopathy and outcome is clearly defined, lessons

Preliminary reports of our findings have been published previously (1992. 11th Meeting of the Society of Magnetic Resonance in Medicine. 237*a* [Abstr.]; and 1992. *Eur. J. Radiol.* 14:128–140).

Address correspondence to Roland Kreis, Ph.D., MR Center 1, Inselspital and University Inselheimmatte, CH-3010 Bern, Switzerland. Phone: 31-632-8174; FAX: 31-382-2486; E-mail: kreis@insel.unibe.ch

Received for publication 26 June 1995 and accepted in revised form 8 December 1995.

J. Clin. Invest.

0021-9738/96/03/1142/13 $2.00
Volume 97, Number 5, March 1996, 1142–1154

1. *Abbreviations used in this paper:* ACLS, acute cardiac life support; Ch, choline; CPC, cerebral performance categories; Cr, creatine; CSF, cerebrospinal fluid; GCS, Glasgow coma score; GM, gray matter; ICU, intensive care unit; Lac, lactate; mI, *myo*-inositol; MRI, magnetic resonance imaging; MRS, magnetic resonance spectroscopy; NA, *N*-acetyl–containing metabolites; NAA, *N*-acetylaspartate; ND, near-drowning; PCr, phosphocreatine; PICU, pediatric ICU; PVS, persistent vegetative state; SPI, spectroscopic prognosis index; TE, echo time; VOI, volume of interest; WM, white matter.

learned in this context may have broader implications for hypoxic encephalopathy in more complex circumstances.

MRS is a noninvasive technique to analyze human cerebral metabolites in vivo. Phosphorus (^{31}P) MRS was used to predict the outcome after neonatal hypoxia from the loss of ATP, accumulation of inorganic phosphate, and intracerebral acidosis (15–17). Proton (^{1}H) MRS reveals the loss of *N*-acetylaspartate (NAA) from the brain in infants suffering cerebral hypoxia (18, 19) and in adults after stroke (20–22), as well as demonstrating the anticipated accumulation of lactate (Lac). Like ^{31}P-MRS, ^{1}H-MRS has been suggested to have prognostic value in both settings. The recent development of quantitative methods of short echo time (TE) ^{1}H-MRS on routine clinical MR scanners (23–27) allows serial comparison of NAA, total creatine (Cr), Lac, and glutamate/glutamine (Glx). NAA is a neuronal marker, the other metabolites can be viewed as cerebral indicators of energy metabolism (Cr) and of cytoplasmic (Lac) and mitochondrial (Glx) redox state. As all of these factors are likely to vary during the recovery after ND, ^{1}H-MRS is ideally suited to document the temporal course of secondary hypoxic encephalopathy and may provide prognostic information in these patients.

The objective of this study applying quantitative ^{1}H-MRS in a series of children after ND was therefore twofold: (*a*) to determine the metabolite profile of secondary hypoxic encephalopathy, including its progression and identification of potential regional variations; and (*b*) to assess its value for the prediction of neurological outcome.

Methods

Human subjects. 16 consecutive admissions to the pediatric ICU (PICU) of Huntington Memorial Hospital for ND (from April 1991 to June 1993) and 52 neurologically normal infants were included in this study. Approval of the Internal Review Board was obtained for all MRS investigations. 14 patients were admitted to the ICU after resuscitation and stabilization at other hospitals, and 2 patients were admitted directly through the emergency department. Table I gives details of age, nature of the submersion accident, GCS, blood pH, and eventual outcome. GCS was recorded both on first contact and on arrival in the ICU. 14 patients had documented cardiac arrest requiring full acute cardiac life support (ACLS) measures, of whom 5 needed defibrillation. The remaining two patients had normal cardiac rhythm by the time of arrival at the hospital. Patients received standard treatment consisting of norcuron/versed/fentanyl neuromuscular block and positive pressure ventilation, inotropic agents, dopamine, and other supportive therapy. After stabilization of cardiopulmonary status, correction of systemic acidosis, and fluid replacement, an initial brain CT was performed.

MRS and magnetic resonance imaging (MRI) procedures. First MRI and MRS examinations were performed in 15 out of 16 patients within 48 h after the accident and repeated within 1–3 d. One patient died before a second MRS examination was possible. In one patient, the first examination was not performed until day 5. In six patients a third MRS examination was done between days 4 and 94. For the determination of progression of hypoxic encephalopathy, the resulting 118 spectra were pooled to yield summed spectra for 1–2, 3–4, and 6-12 d (gray matter [GM]) and 5–8 d (white matter [WM]) after injury. 3 of the 37 MRS sessions were performed without absolute quantitation. Normative curves for age-matched comparison had been obtained from 52 children between a few days and 14 yr old (28). Individual data from 16 children in the age range of our ND patients and presumed to be neurologically normal are included in some of the figures to indicate normal variation.

Patients were transferred to the MRS Center by a transport team including an intensive care nurse, respiratory therapist, and pediatric intensive care physician. During MRS procedures, artificial manual ventilation was continued via a 3–4-m tube, fitted with a T-piece to reduce dead space. Intravenous infusions were continued via elongated i.v. lines, with mechanical syringes securely mounted 4 m from the magnet bore. ECG monitoring was discontinued and vital signs were observed via a pulse oximeter. The intensive care nurse and respiratory therapist remained with the patient throughout.

MRI (T_1- and fast-spin-echo T_2-weighted sequences) was performed in the axial plane to identify edema, brain swelling, or cortical atrophy, and to select the regions of brain for MRS. Two locations were chosen with potentially differing sensitivity to hypoxia: one in the occipital GM of the posterior parietal lobes (above the calcarine fissure and across the midline), and the other in the parietal WM. Voxels were 10–12 cm^3 ($\sim 2 \times 2 \times 2.5$ cm) and care was taken in placement to permit repeated assays of nearly identical volumes (Fig. 1). Cerebral locations of prime neurological interest, like hypothalamus or mid-brain, were deemed unsuited on grounds of their small size and irregular shape. A complete quantitative MRS evaluation for both brain locations including MRI was completed in 65 min.

The technique of quantitative, short TE MRS has been described in detail elsewhere (23, 24, 28, 29) and will only be outlined here. All spectra were acquired with a STEAM localization sequence (TE 30 ms, middle time 13.7 ms, repetition time 1.5–5 s) on a GE Signa 1.5T clinical MR scanner. The partial volumes of brain water, cerebrospinal fluid (CSF), and dry matter of the volume of interest (VOI) were determined from a T_2 determination of the water signal. The signal from an external reference standard was used for absolute quantitation.

Evaluation of MRS results. Spectra were evaluated in two different ways: first, on the basis of relative (nonquantitative) peak ratios with respect to the Cr resonance (29) without any further corrections, but expressed relative to normative age-relating curves (28); second, in the form of absolute tissue concentrations (24, 28), again expressed as percentages of the age-related normal level. Relaxation times and broad baseline contributions were not measured in ND patients but were assumed to be similar to those in the normal population. Potentially altered metabolite relaxation times are not expected to change any of the major findings in this paper, first because the acquisition parameters are insensitive to relaxation time changes, second because simultaneous increases in T_1 and T_2, as might be expected in edema, would be counteracting, and third because some metabolites appear unaltered after ND. The displayed spectra were all scaled to the signal from tissue water. Direct comparison of peak areas is possible and yields a molal correspondence (24). Because of the different spectral processing and normalization, peak ratios cannot be compared directly with ratios of absolute concentrations.

To clearly identify the effects of ND, patient spectra were summed, reducing the effects of interindividual differences and of varying residual water signal or outer-volume lipid contamination. Difference spectra (30) with respect to averaged control spectra were compared with spectra from aqueous solutions of the pure metabolites to identify changes in the metabolite profile. The strong negative contributions to the difference spectra due to the deficit in NAA made it difficult to identify other components in the spectral region from 2.0 to 2.6 ppm. Cancellation of these negative peaks using NAA solution spectra proved inadequate. Instead, we subtracted an in vivo spectrum obtained from normal age-matched subjects, from which spectral contributions of high molecular weight (i.e., short T_1) components had first been eliminated using acquisitions at differing repetition rates (compare with reference 31).

Because of overlap with lipid resonances, Lac quantitation was done as follows. Each spectrum was Lorentz-Gauss transformed (29) and scaled using the absolute size of Cr. An identically treated normal spectrum (average from young healthy adults) was subtracted. Residual broad contributions were removed by high frequency filtering of the difference spectrum. Finally the in vivo spectrum was multiplied with an equally treated in vitro Lac spectrum to yield a value for

Table I. Summary of Clinical Data of ND Patients

Patient	Age	Sex	Site	Full arrest (ER)	Resuscitation (ER)	GCS (ER)	GCS (PICU)	Pupils (ER)	Pupils (PICU)	ABG (ER)						Outcome on discharge	CPC
										pH	PCO_2	PO_2	Sat	HCO_3	BE		
	yr										*KpA*	*KpA*	*%*	*meq/liter*			
Group 1: good outcome																	
1	6 5/12	M	River	Yes	ACLS+DF	3	7	NR	R	6.56	104	71	NA	9.3	NA	Excellent	1
2	3 5/12	M	Pool	No	Intubation alone	4	4	R	R	7.06	25	281	NA	6.8	NA	Excellent	1
3	3 4/12	M	Pool	Yes	ACLS	3	5	NR	R	6.75	28	597	100	3.9	−33	Alert, playful; unsteady gait (day 11)	2
4	2 1/12	M	Pool	Yes	ACLS	6	6	R	R	7.12	30	41	0.61	9.8	−18	Excellent (day 3)	1
5	3 6/12	M	Pool	No	None	5	5	R	R	6.98	54	69	0.80	12.8	−20	Excellent (day 5)	1
Group 2: vegetative outcome																	
6	2 6/12	M	Pool	Yes	ACLS	NA	6	NR	R	7.26	NA	NA	NA	NA	NA	Vegetative	4
7	6 5/12	M	Pool	Yes	ACLS	3	5	NA	R	6.80	62	219	1.00	2.9	−26	Vegetative	3/4
8	1 7/12	M	Pool	Yes	ACLS+DF	3	3	NR	R	6.79	31	437	1.00	4	−27	Vegetative	4
Group 3: died																	
9	1 6/12	F	Pool	Yes	ACLS	3	3	NR	R	6.8	64	112	1.00	9.2	−2.5	Disconnected (day 12)	5
10	2 10/12	M	Pool	Yes	ACLS	3	3	NR	R	6.6	144	19	NA	25	38	Disconnected (day 3)	5
11	7/12	F	Bathtub	Yes	ACLS	3	5	NR	R	6.7	61	70	1.00	7	NA	Disconnected (day 14)	5
12	2 8/12	M	Pool	Yes	ACLS+DF	3	5	NR	R	6.57	169	NA	NA	NA	NA	Disconnected (day 5)	5
13	6 6/12	M	Pool	Yes	ACLS+DF	3	3	NR	R	6.61	32	614	1.00	3	−38	Disconnected (day 3)	5
14	1 9/12	M	Pool	Yes	ACLS	3	3	NR	R	6.9	79	77	0.82	15.8	−18	Expired (day 6)	5
15	1 10/12	F	Pool	Yes	ACLS	3	3	NR	NR	6.94	38	496	1.00	NA	−22	Disconnected (day 5)	5
16	1 4/12	M	Pool	Yes	ACLS+DF	3	4	NR	R	6.58	95	NA	NA	NA	NA	Disconnected (day 7)	5

ER, emergency room; *ABG*, arterial blood gases; *Sat*, O_2 saturation; *NR*, nonreactive; *R*, reactive; *DF*, defibrillation.

Lac by integration over a range of 0.19 ppm. (For the combined prognostic index, these Lac values were normalized by adding a constant and dividing by the normal mean [resulting range 0.8–2.6]).

Clinical outcome. Two criteria are used in this paper to define outcome after ND. The simpler is the division into good and bad outcome; the other is the cerebral performance category (32) (CPC, Table I), defined as follows: CPC 1 = good cerebral performance; CPC 2 = moderate cerebral disability; CPC 3 = severe cerebral disability; CPC 4 = PVS; and CPC 5 = brain or clinical death. Thus, the above division into good and bad outcome corresponds to CPC 1–2 vs. 3–5. A partition into three groups (good vs. PVS vs. died) corresponds to CPC 1–2 vs. CPC 3–4 vs. CPC 5.

Statistics. Significance of differences between groups was tested using multivariate analysis of variance and pairwise comparisons based on the mean square error from ANOVA. A Bonferroni correction for six comparisons (normal vs. good and bad outcome on days 1–2 and 3–4, as well as distinction between good vs. bad outcome on days 1–2 and 3–4) was included. Significance was expressed when $P \leq 0.01$ to additionally compensate for multiple variable testing. Non-parametric tests included Kendall τ_b correlation testing (Systat for Windows, Version 5, SYSTAT Inc., Evanston, IL, 1992).

Results

In keeping with the double goal of this paper to characterize MRS reflections of hypoxia after ND and to investigate the potential of MRS for prognosis of outcome, the MRS results are presented in two corresponding parts, the first dealing mostly with averaged spectra, the second relying on individual data. The sections on MRS results are followed by paragraphs on morphologic changes and clinical results.

Cerebral metabolic alterations after ND. The most obvious changes in the cerebral ^{1}H-MR spectrum after ND are illustrated in Fig. 2 for a single case of a 3-yr-old ND patient. 48 h after admission to ICU, i.e., many hours after successful reperfusion and oxygenation, there is an increase in Lac, decreases

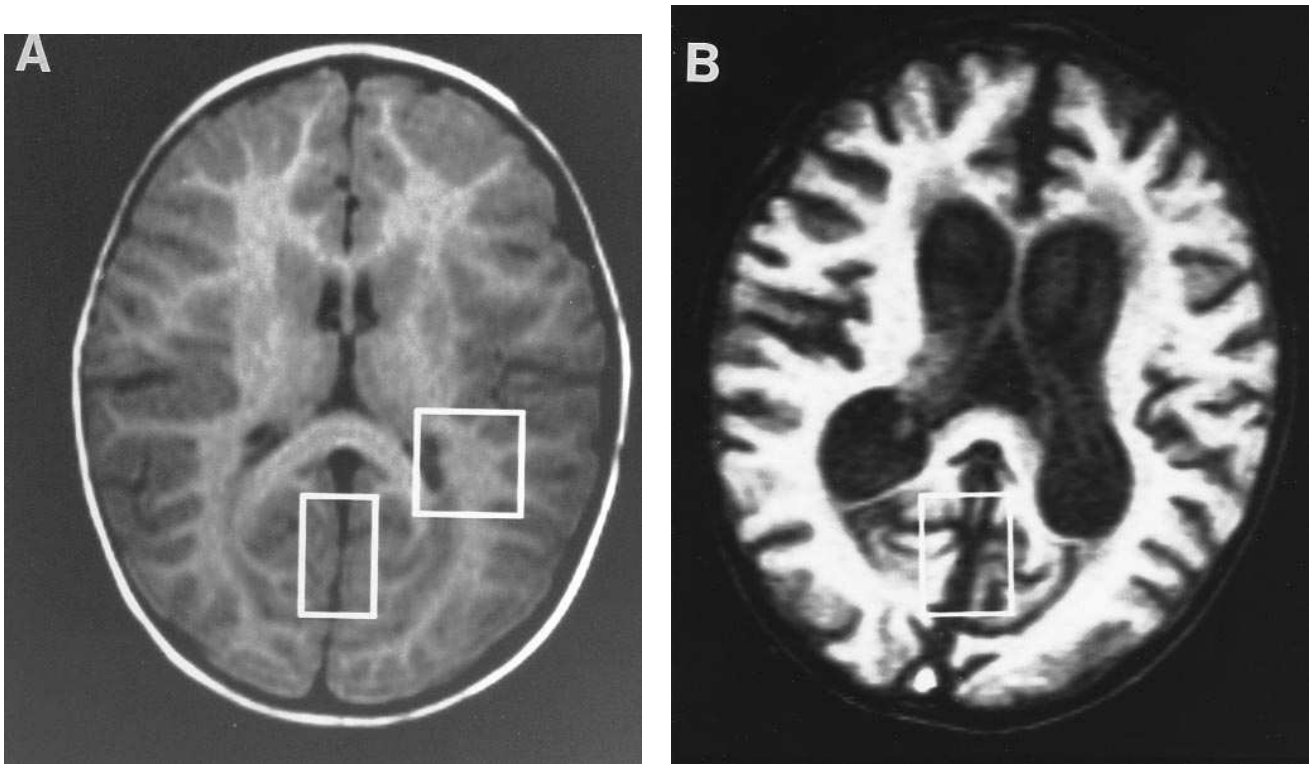

Figure 1. MR images (T_1-weighted with TE 20 ms, repetition time 600 ms) showing the inferior bounds of the typical location of the regions of interest studied as well as the morphologic changes after ND as detected by MRI. MRI appears normal early after ND (*A*) but reveals considerable cerebral atrophy 3 mo after ND (*B*).

in NAA and Cr, and alterations in the spectral regions of glutamine (Gln) and glutamate (Glu) (β- and γ-protons at 2.0–2.5 ppm and the α-protons at 3.75 ppm). Negative findings include the absence of significant lipid accumulation, of ketone bodies (acetoacetate or β-hydroxybutyrate), or of a distinct increase in Glu compared with Gln.

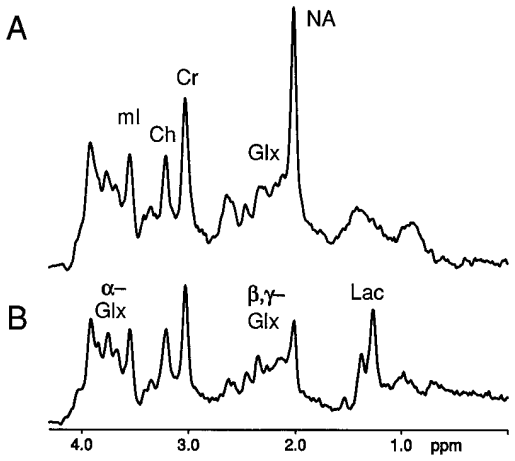

Figure 2. Cerebral ^{1}H-MR spectra of occipital GM in a 3-yr-old boy 48 h after ND (*B*) compared with a control spectrum of a healthy age-matched subject (male, 4 yr) in *A*. The spectrum of the patient who died 70 h after injury is characterized by a dramatic loss of NAA (2.0, 2.6 ppm), a decrease in Cr (3.0 and 3.9 ppm), a large increase in Lac (1.3 ppm), and changes in the resonances of Glu and Gln (3.75, 2.0–2.5 ppm).

These spectral changes in a single subject are confirmed in spectra obtained from groups of patients (Fig. 3). The difference spectrum in Fig. 3 *C* shows very clearly the excess in cerebral Lac (positive doublet at 1.3 ppm) and negative peaks for NAA (methyl protons at 2.0 ppm and methylene signals at 2.6 ppm), Cr (3.0 ppm), and also *myo*-inositol (mI, 3.6 ppm). The difference spectrum in Fig. 3 *D*, which was corrected for the NAA deficit as described in Methods, suggests that the spectral alterations from 2.1 to 2.5 ppm reflect increased Gln (Fig. 3, *D* vs. *E*), accompanied by some reduction in Glu (compensated for in Fig. 3 *D* by the added control spectrum).

Progression of metabolic deterioration in two brain regions. The striking progression of metabolic damage is illustrated in Fig. 4 for both GM and WM locations. Averages of all spectra from the bad outcome group are shown, classified by interval since injury. The initial decrease in NAA present after 1 d progresses over the ensuing days, and in GM NAA is only $\sim$ 30% of normal after 1 wk. The effects on Cr are not as conspicuous, but it is still evident that Cr also drops over days after ND. Abnormal Lac and Glx peak intensities appear on day 1 in GM and develop to maximum extent around day 4. The choline (Ch) peak intensity, which is very susceptible to alterations in WM/GM composition of the VOI, changes remarkably little.

Comparison between WM and GM spectra in Fig. 4 indicates that loss of NAA and Cr and increase in Lac are common to both locations, but are more expressed in GM of parieto-occipital cortex than in WM of parietal cortex, particularly on

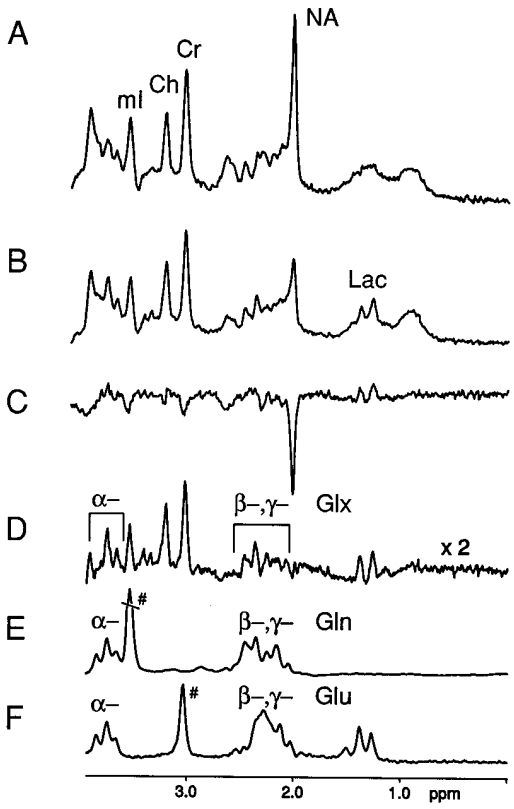

Figure 3. Average ^{1}H-MR spectrum from all patients with bad outcome investigated 3–4 d after submersion (*B*), compared with an averaged spectrum obtained from a group of age-matched control subjects (*A*). The difference between patient and control spectra in *C* illustrates the metabolic alterations in secondary hypoxic encephalopathy: decreases in cerebral NAA, Cr, and mI contents and the appearance of Lac. Additionally there are specific changes in the spectral region of β-,γ-Glx which are analyzed in *D*, where the large NAA deficit was canceled using a specially prepared normal spectrum. The resulting spectrum resembles more closely the spectrum of Gln (*E*) than the one of Glu (*F*). Peaks marked # are chemical shift references (creatinine, glycine) and the spectrum in *F* additionally contains Lac (1.3 ppm).

days 1–2. The spectral changes of Gln and Glu, prominent in the GM spectra on days 1–2 and 3–4, are hardly discernible in any of the summed WM spectra. The concentration difference in Ch between WM and GM locations known for healthy subjects is conserved after ND.

MRS changes in relation to clinical outcome. Fig. 5 demonstrates that, at least in single cases, there is a striking correlation between spectra and outcome already on day 2 after the immersion accident, while the patients are still in coma and on ventilator support. The GM spectrum originating from the patient who fully recovered (Fig. 5 *B*) is much closer to normal (Fig. 5 *A*) than the one from the patient who subsequently died (Fig. 5 *C*).

The correlation between extent of spectral abnormalities and outcome also holds for patient groups, as evidenced by Fig. 6 and the *t* test probabilities in Table II. On days 1–2 (Fig. 6 *A*), a reduction in *N*-acetyl–containing metabolites (NA) is readily discerned in the GM spectrum of patients with good outcome, but is much more severe in patients who became vegetative, or who died. Similarly, Cr showed a greater decrease in patients who became vegetative or died. At this early time point, Lac is clearly identifiable only in the spectra of patients who subsequently died. These distinctions became much more marked after 3–4 d (Fig. 6 *C*). An elevation in β-,γ-Glx, which was not discernible in the good outcome spectrum, was clear in both other groups at this time. The spectra from WM (Fig. 6, *B* and *D*) show similar trends, but elevations in Lac and β-,γ-Glx appeared in WM only after 3–4 d, and only in those groups of patients which did not do well.

Only some of the differences which are clearly distinguishable in the summed spectra reached statistical significance (Table II). Other very clear differences between the sum spectra (e.g., Lac in GM) were judged insignificant compared with the Bonferroni corrected mean square error in a multivariate analysis. Nevertheless, NA/Cr was significantly decreased on days 1–2 and 3–4 and was significantly lower in bad outcome than in good outcome. Cr was significantly reduced in patients with bad versus good outcome in GM and lower than the norm in WM. The increases in Glx also reached statistical significance as indicated in Table II.

Prognosis with MRS after ND. To be of prognostic value, differences in MRS must be discernible in individual patients. A representation of the time course of individual data for the GM location is presented in Fig. 7 and discussed in the following paragraphs.

NA/Cr is reduced in all patients, even at the earliest time points studied, and falls progressively thereafter (Fig. 7 *E*). There is a readily discernible difference between the extent of this decline in individual patients with good outcome (*open squares*) compared with those who did poorly (*filled triangles*) or died (*filled squares*). On the basis of NA/Cr and the rate of its decline, good versus bad outcome is defined in every patient on days 1–4. In only one patient with poor outcome (patient 11; Fig. 7 *E*) is there any recovery of NA/Cr.

Patients with poor outcome could not be unequivocally identified from NA on day 1 (Fig. 7 *A*). In only 7 of 11 patients was there a clear reduction in NA at the earliest time point. NA then generally falls and appears to be predictive of outcome from day 2 onward. The measured NA concentration may be overestimated in patients who show a marked increase in Glx, due to spectral overlap, hiding an even earlier and more dramatic loss of NA. The Cr concentration was reduced in most patients at the earliest time point, and in poor outcome cases it generally continued to fall. In 4 out of 5 patients in whom outcome was good and quantitative measurements are available, Cr rose over the same time period. Discrimination on the basis of Cr alone was not possible on day 1 and there remained considerable overlap between good and poor outcome on days 2–4.

In some patients, Lac increased markedly from an already elevated level on day 1 or 2 to the maximum measured values on day 4. The highest Lac peaks correspond to an estimated concentration of $\sim$ 5 mM. Those patients demonstrating an excess of Lac in the spectrum from occipital GM invariably did poorly (Fig. 7 *C*), but normal Lac content did not guarantee good outcome. An elevated cerebral Glx/Cr ratio in GM can be used to predict outcome, despite a fairly large measurement inaccuracy. On days 1 and 2 almost all patients with poor outcome could be distinguished from those with an eventual good outcome. Glx paralleled Lac to reach highest values 3–4 d after ND.

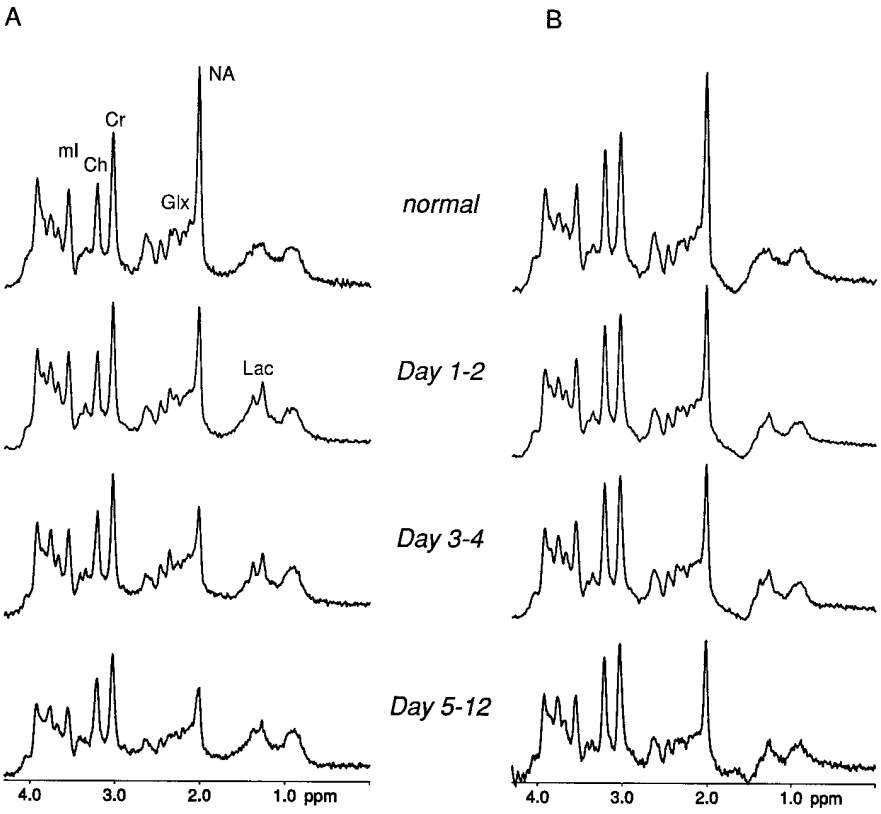

Figure 4. Averaged spectra documenting the changes in total metabolite content occurring in patients with bad outcome over the course of several days after ND. The decrease in cerebral NAA occurs faster and to a larger extent in GM (*A*) compared with WM (*B*). The accumulation of Lac is also more expressed in GM.

The MRS findings in WM were very similar. However, on day 1 NA/Cr was generally within normal limits. By day 2 only, patients with poor outcome showed NA/Cr below normal and below most of the patients with good outcome. While NA/Cr and NA consistently fell over time, overlap between the results in patients with good and poor outcome persisted, and the clear separation noted in GM was absent. As in GM, Lac reached its highest values in patients with poor outcome. Glx/Cr increased progressively in WM as it did in GM, but with incomplete separation between good and poor outcome.

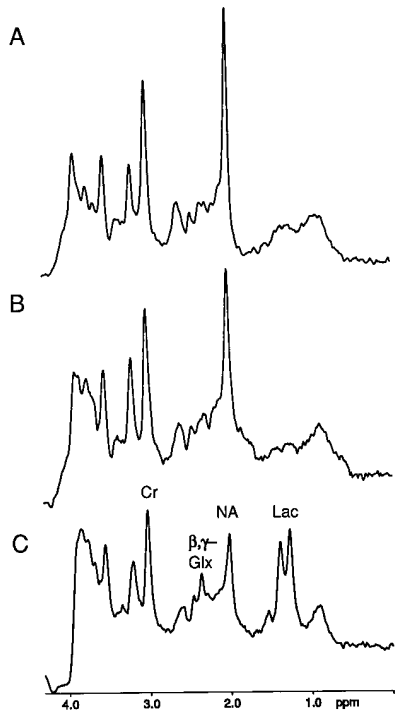

Figure 5. Cerebral ^{1}H-MR spectra of occipital GM demonstrating that final outcome is reflected by the severity of spectral changes 2 d after submersion. *A* shows a normal control subject (female, 4 yr); *B* shows a 2-yr-old boy who recovered fully; and *C* shows a 6-yr-old boy who died 3 d after ND. Spectral changes in NA, Cr, Glx, and Lac are dramatically more expressed in the bad outcome case in *C*. The relatively high Ch peak in *B* is age related.

Because of the large individual spread and limited number of patients for each group, a temporal trend was only modeled for the NA/Cr ratio which is least affected by measurement inaccuracy and potential changes in water content. For the bad outcome cases, the decline in NA/Cr of GM from normal (used as day 0) to day 12 can be described by a double exponential decay, where one component, representing $\sim$ 40% of the signal, falls rapidly with a decay time of little above 1 d, and where a second component with 60% of the signal shows a much slower decay of several tens of days, i.e., almost constant amplitude over the observed time span. In WM the NA/Cr signal decay can be well described by a mono-exponential decay (decay time of 18 d). If a bi-exponential decay model is imposed and GM and WM data are fitted together, the resulting decay times are close to the original GM values (1.2 d for the fast and 30 d for the slow decay). The components defined in this way have different proportions in GM and WM: 34:66% for fast versus slow components in GM versus 14:86% in WM.

Prognosis from multiple variables in MRS. Because each of the MRS variables confers increasing sensitivity upon the definition of outcome, we combined the most discriminating measurements for each patient and each time point (Table III and Fig. 8) to obtain a spectroscopic prognosis index (SPI): $SPI = NA \cdot Cr \cdot (NA/Cr)/(Lac\% \cdot \beta\text{-},\gamma\text{-}Glx)$; where *NA*, *Cr*, and β-,γ-*Glx* are in absolute units, and *Lac%* is a normalized measure of Lac (see Methods). As can be readily seen, SPI is superior to any of the individual metabolite assays, when measured in GM (Fig. 8 *A* and Table III). If an arbitrary, time-dependent

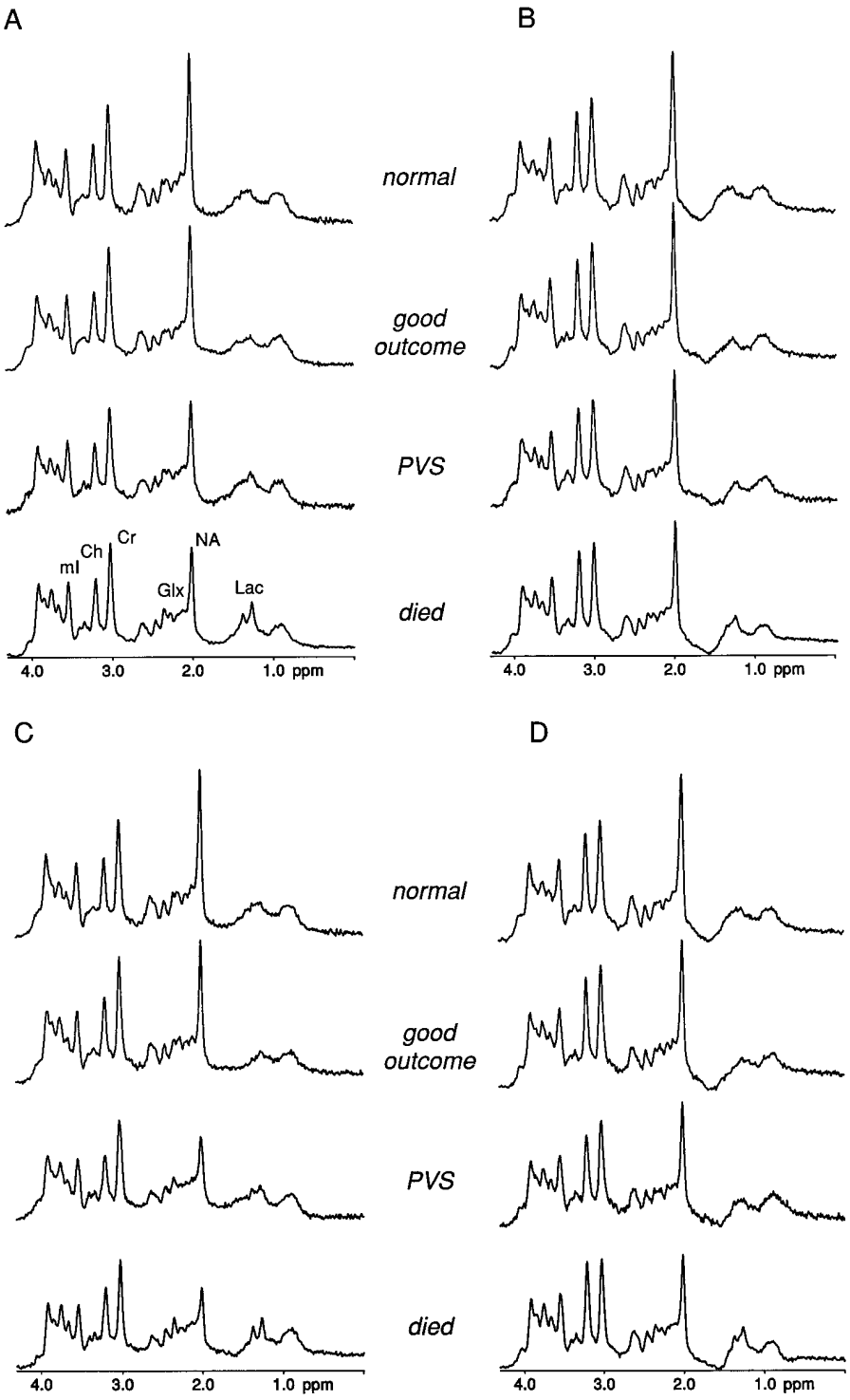

Figure 6. Averaged ^{1}H-MR spectra in victims of ND grouped according to eventual outcome and time after submersion (*A* and *B* at 1–2 d; *C* and *D* at 3–4 d after ND). Spectra in *A* and *C* originated from the GM location; those on the right (*B* and *D*) from the WM VOI. In all panels the largest deviations from normal occur in the spectra from ND victims who did not recover fully. There is no clear distinction between patients who died and those who developed a PVS.

threshold between good and bad outcome is chosen, 100% accuracy is achieved from day 1 to day 4. The one false negative (prediction of good outcome, in a patient who subsequently did poorly) on day 8 had already been correctly grouped on two previous examinations (patient 11). There were no false positives, when defined by this series of measurements in GM from day 1 up to and including day 12. If the borderline between good and bad outcome is set time-independently at a value corresponding to the mean − 2 SD in the control group, then reliable distinction between the two main outcomes is only achieved by day 3. Two early measurements in bad outcome cases would stand as false negatives. Three further bad outcome cases on days 1–2 would be on or right below the threshold and two good outcome cases would be little above the borderline on day 4, the latter indicating that there is some metabolic damage also in good outcome cases. Greater sensitivity was conferred by using sequential results; thus, the trend usually further separates bad from good outcome results. The two false negative predictions clearly converted to the correct predictive result on the second MRS examination.

Table II. Summary of ^{1}H-MRS Data, Grouped According to Outcome, Examination Day, and Location

Outcome Days	Norm Mean±SD	Good 1–2 Mean±SD	*P**	Good 3–4 Mean±SD	*P**	Bad 1–2 Mean±SD	*P**	*P*‡	Bad 3–4 Mean±SD	*P**	*P*§
Gray matter											
NA	100±17	89±9		88±13		73±17	< 0.01		64±12	< 0.001	
Cr	98±6	94±5		106±11		86±11			80±16	0.02	< 0.01
Ch	97±14	91±18		111±17		83±10			83±16		< 0.05
mI	88±23	93±19		107±29		96±35			72±29		
α-Glx	99±23	96±12		127±19		108±29			101±18		
β-,γ-Glx	108±23	96±15		117±11		111±15			110±11		
Lac	−0.11±0.29	−0.24±0.10		0.00±0.18		0.63±1.08			0.60±0.78		
NA/Cr	96±9	82±2	0.02	76±5	0.004	70±9	< 0.001	< 0.05	57±6	< 0.001	< 0.01
α2	0.10±0.07	0.04±0.02		0.07±0.01		0.04±0.01	< 0.01		0.05±0.02		
White matter											
NA	100±12	88±13		85±11		81±10	0.001		75±10	< 0.001	
Cr	101±10	101±7		101±8		92±09	< 0.05		88±03	< 0.01	
Ch	96±08	88±7		91±16		86±10			87±11		
mI	96±21	112±32		105±25		95±13			109±19		
α-Glx	108±9	126±12	0.02	130±16	< 0.01	114±11			113±9		
β-,γ-Glx	119±17	109±9		118±23		126±15			132±13		
Lac	−0.17±0.20	−0.15±0.10		−0.14±0.24		0.15±0.49			0.28±0.47	< 0.05	
NA/Cr	98±10	88±7		84±6	0.03	85±10	< 0.01		76±4	< 0.001	
α-Glx/Cr	1.08±0.12	1.25±0.08	0.02	1.28±0.05	< 0.01	1.24±0.13	< 0.01		1.29±0.10	< 0.001	
β-,γ-Glx/Cr	1.08±0.14	0.99±0.08		1.08±0.12		1.26±0.13	0.01	< 0.01	1.37±0.13	< 0.001	< 0.001
α2	0.05±0.03	0.04±0.02		0.05±0.01		0.03±0.02			0.06±0.05		

Values represent percent values of the age related norm defined in reference 28, except for Lac (arbitrary units) and α2 (percent of CSF in VOI). As an example, normal metabolite concentrations as defined by the normative curves are given for a 5-yr-old child: NAA 8.8 in GM and 7.6 in WM; Cr 8.3 and 6.6; Ch 1.3 and 1.6; mI 7.4 and 6.9 (in mmol/kg wet weight). *P with respect to comparison to the normal group; ‡P with respect to comparison between good and bad outcome on days 1–2; §P with respect to comparison between good and bad outcome on days 3–4.

A similar plot is presented in Fig. 8 *B* for parietal WM. While the same trends are seen as in GM, the segregation of patients was less satisfactory. Fig. 8 *D* demonstrates that the metabolic damage in GM and WM occurs in parallel, with the WM changes being smaller. For an optimal SPI, they were combined with equal relative weights (Fig. 8 *C*). However, a distinction between patients who subsequently died and those with PVS could not be achieved with this index.

Morphologic changes after ND. Morphologic cerebral changes after ND include brain swelling (edema) and, at a later stage, cortical atrophy. Indications of these alterations were found with quantitative MRS of water and by MRI. Although cerebral edema is considered a cardinal feature of early hypoxic encephalopathy, direct assays of brain water did not show a significant increase in the ND population compared with normals (water content = 0.73±0.03% in ND at days 1–2 vs. 0.74±0.02 in normals, $P > 0.05$). In contrast to the constancy of brain water, the "atrophy index," α2 (23), was significantly reduced in occipital GM on days 1–2, consistent with brain swelling. α2 recovered and was not significantly different from normal by days 3–4 ($P = 0.06$). In three out of six measurements made after day 5, α2 exceeded normal, indicative of posthypoxic cortical atrophy.

All MRI examinations performed within 24 h ($n = 7$) were normal and only 2 of 11 examinations within the first 48 h were abnormal: loss of gray-white contrast in one and "mild cerebral swelling" in the other indicated cerebral edema in children who subsequently died. Two of six MRI examinations between days 3 and 4 were mildly abnormal, with slight ventricular dilatation in one (good outcome) and loss of gray-white contrast in the other (died). Later, structural damage was obvious in three out of five patients: modest ventricular dilatation on day 8 in a child who subsequently died; focal thalamic changes on day 12 in a child with PVS; and gross ventricular dilatation on day 94, in another child with PVS (Fig. 1). The other two patients with late follow-up exams showed normal images. In summary, MRI gave little early indication of final outcome; however, late structural damage is clearly visible in patients with unfavorable outcome.

Clinical determinants of outcome after ND. The present series conforms to earlier studies of ND, with 5 out of 16 patients classified as good outcome (31%) and 11 out of 16 (69%) as bad outcome. The bad outcome group was further divided into those who survived in a PVS ($n = 3$) and patients who died ($n = 8$) within 14 d of ND (6.9±2.6 d). The CPC scores are listed in Table I. Mean GCS after stabilization in the PICU was 5.4 for good outcome (range 4–7) and 3.9 for bad outcome (range 3–6). However, the range of GCSs showed overlap between the groups such that, with a threshold of 4.5, 3 out of 10 false negative (with respect to a prognosis of bad outcome; i.e., incorrectly predictive of good outcome) and 1 out of 4 false positive (incorrectly predictive of bad outcome) results were observed using GCS values after stabilization. (For proper comparison with MRS predictions, two patients with nonquantitative early MRS examinations were disregarded. Inclusion of these patients yielded 4 out of 11 false negative and 1 out of

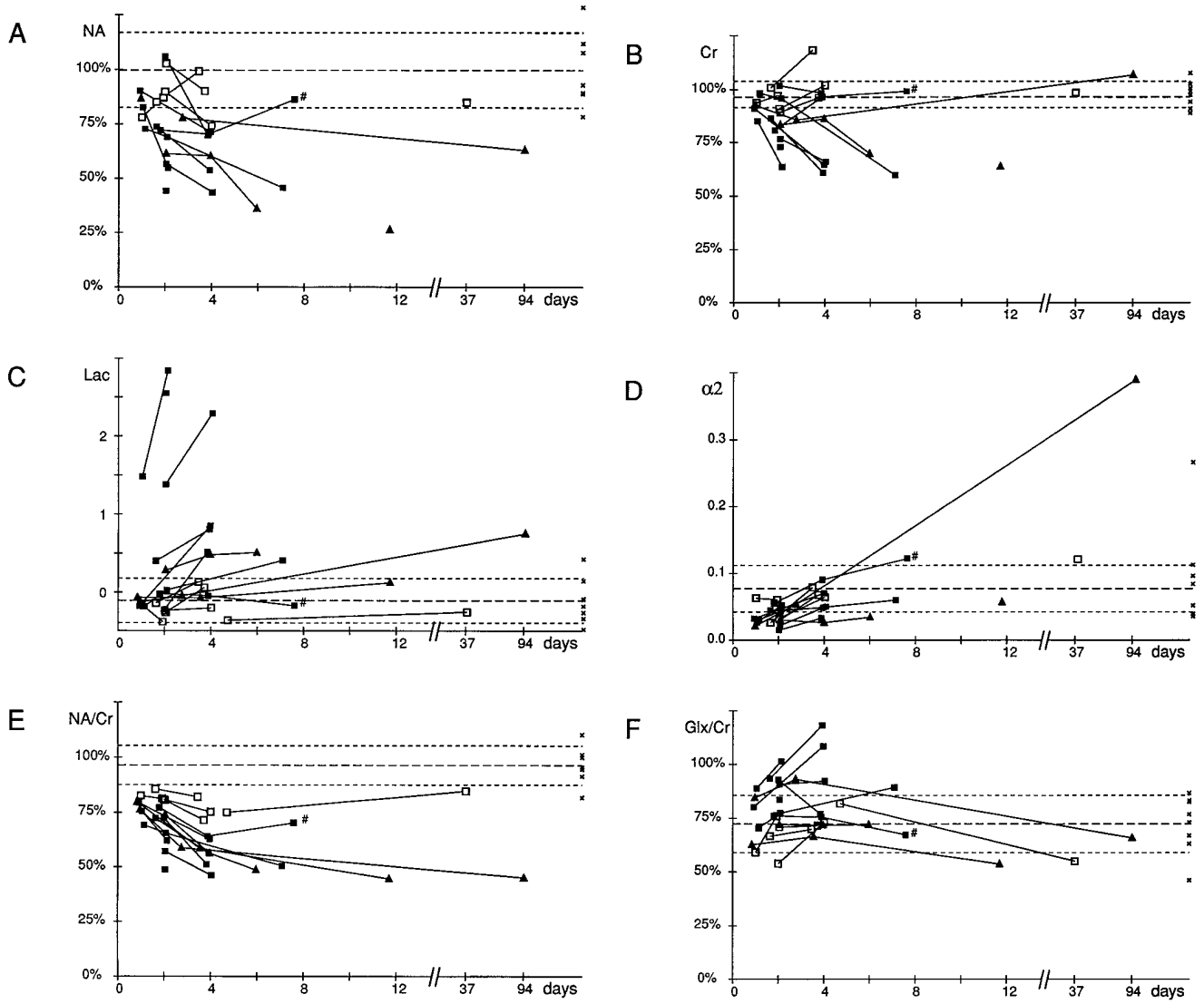

Figure 7. Time course of the most affected metabolites in 16 patients after ND. The values for NA, Cr, NA/Cr, and β-,γ-Glx/Cr reflect percentages with respect to the age-related norm (28). Lac represents a semiquantitative measure of Lac content, whereas α2 indicates the relative proportion of CSF in the VOI and is sensitive to edema and atrophy. All data originate from the GM location. Open squares represent data from patients with good outcome, filled triangles and filled squares stand for data from patients in a PVS and those who subsequently died, respectively. Temporal evolution in single subjects is indicated by connecting lines. Normal data and normal ranges are represented by crosses and dashed lines for the mean and mean±1 SD in the control group. The case of patient 11, who judging from MRS improved but died on day 14, is marked by #.

5 false positive.) A clearer distinction is obtained using GCS values on arrival in the emergency room. With a threshold of GCS 3.5, no false negative but one out of four false positive is recorded (two out of five false positives including all cases).

Minimum blood pH, which has been suggested as predictive of outcome, was 6.78 in the bad outcome group (range 6.57–7.26) and 6.90 in the good outcome group (range 6.56–7.12). Again the overlap is great; applying a threshold of pH

Table III. SPI Grouped According to Outcome, Examination Day, and Location

Outcome Days	Norm	Good 1–2		Good 3–4		Bad 1–2			Bad 3–4		
	Mean±SD	Mean±SD	*P**	Mean±SD	*P**	Mean±SD	*P**	*P*‡	Mean±SD	*P**	*P*§
SPI (GM)	91±20	78±10		57±8	< 0.05	34±18	< 0.001	< 0.001	21±11	< 0.001	< 0.05
SPI (WM)	85±24	72±20		60±4		44±14	< 0.001	< 0.05	31±10	< 0.001	
SPI (WM+GM)	87±16	75±8		58±5	< 0.05	39±16	< 0.001	< 0.001	26±10	< 0.001	< 0.01

Definition of * ‡ § as in Table II.

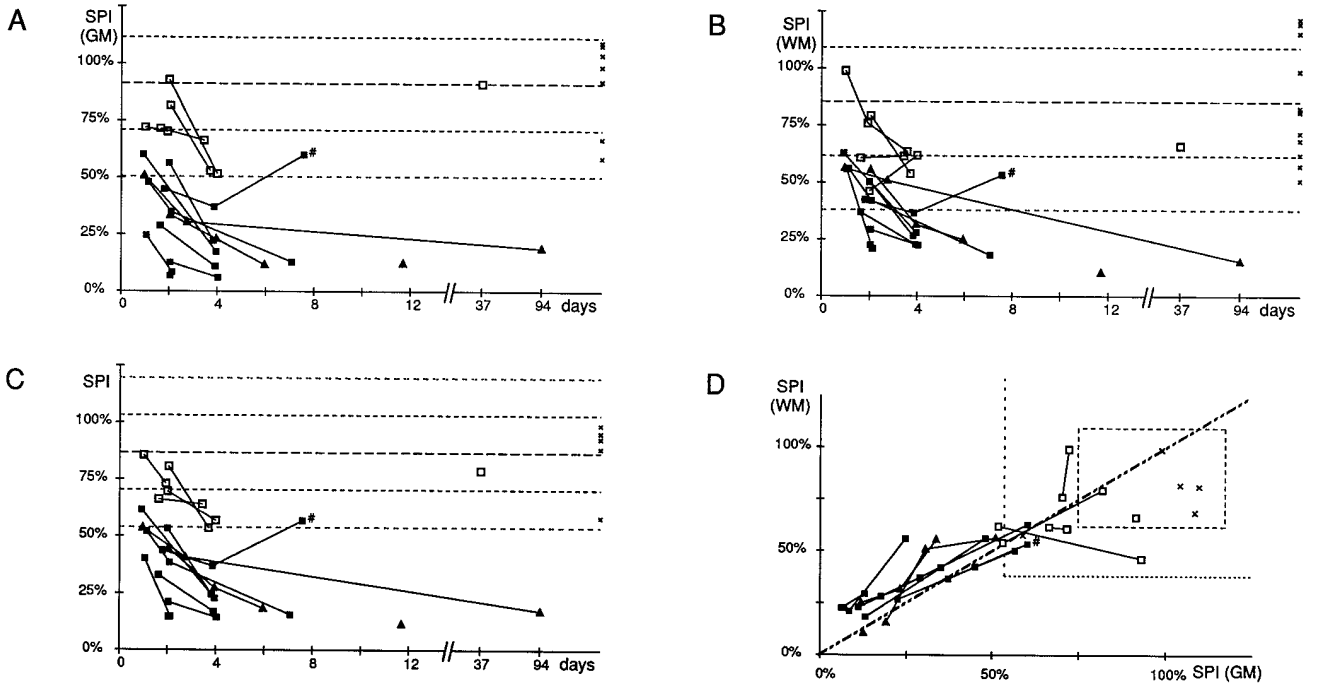

Figure 8. SPI combines different spectral quantities to optimize the potential for prognosis of eventual outcome using ^{1}H-MRS. *A* contains data from NA, Cr, NA/Cr Lac, and β-,γ-Glx/Cr from the GM volume and achieves a promising separation of data from good and bad outcome groups, even early after ND. SPI defined on the basis of WM data is less discriminant (*B*). Optimal distinction is achieved combining WM and GM data, represented in *C*. *D* illustrates the correlation of the severity of cerebral metabolite changes in the investigated regions of GM and WM. Dashed lines indicate the mean, mean±1 SD, and mean±2 SD in the control group.

7.0 results in no false negative (1 out of 11 including all cases), but 2 out of 4 false positive values (3 out of 5 including all cases). Neurological evaluations performed later were not considered, because of results obscured by the use of sedatives and muscle relaxants for therapy.

Discussion

Metabolic effects of hypoxic encephalopathy. The reactions of the brain when deprived of normal oxygen supply are of great complexity and not completely understood, partly because of the interfering effects of ischemia and inadequate reperfusion. In the present study, quantitative ^{1}H-MRS was used to analyze metabolic events after cerebral hypoxia due to ND. The detailed results of the study discussed below should be viewed in the light of the anticipated histopathological and biochemical events involved, and the inherent limitations of the method. It is important to note that MRS is insensitive to small metabolic changes on the cellular level unless reflected on a macroscopic scale and that MRS measures average tissue content, not differentiating between cell types or extracellular space, but excluding CSF spaces. Therefore, brain edema (e.g., initial astrocytic edema) is not detected if caused by a redistribution of fluid between intra- and extracellular space within the VOI. Neuronal cell damage (microvacuolization), as described as one of the first steps in the hypoxic cascade of events (4–6, 33, and references therein), will lead to a spectral decrease in neuronal metabolites only, if cell contents are removed from the investigated VOI, which may not happen instantaneously, but certainly much earlier than the dissolution of the whole neuron as evidenced by histopathology. Tissue content of metabolites not primarily located in affected cells will change when the surviving cells condense due to vacated neuronal space, or if other cell populations intrude. Metabolite concentration changes may also reflect changes of chemical equilibria in surviving cells due to altered redox or osmotic conditions, for example. Furthermore, cerebral metabolites synthesized in other organs may change in concentration because their de novo synthesis could be reduced after hypoxia.

The most striking effect of ND on the brain ^{1}H-MR spectrum is the progressive loss of NAA. This confirms the selective vulnerability of neurons, because NAA has been shown to be almost exclusively restricted to neurons in mature brain (34–36). Loss of NAA has been reported to occur within hours in stroke (20, 21, 37) and in neonatal hypoxia (19, 38). Here we provide evidence that in ND, after an initial loss within the first 24 h (∼ 20% in GM), the NAA content continues to decrease for days after the original hypoxic insult (to as low as 25%).

Another noticeable consequence of ND is the loss of total Cr from both WM (to 75%) and GM (down to 60%) regions of the brain. From ^{31}P-MRS in asphyxiated infants (39) and experimental hypoxia in piglets (40), it is known that phosphocreatine (PCr) is restored fully within hours of an hypoxic insult, but may diminish subsequently over days in what has been called "secondary cerebral energy failure." The present study confirms this to be a feature of human brain. ^{1}H-MRS is unable to directly assay PCr, but assuming that the simultaneously observed Lac is a reflection of an increase in NADH/NAD, PCr probably falls out of proportion to the total Cr pool. Loss of total Cr implies either reduced synthesis in liver and kidney, or "leakage" from damaged brain cells. There is evidence that Cr is found in both neurons and glial cells,

though possibly in different proportions (35). Therefore, the Cr loss may be viewed as another reflection of neuronal cell death.

A surprising feature of this study is the prevalence of changes in the tissue contents of Gln and Glu early during recovery from hypoxia. The spectral changes related to β-,γ-Glx indicate an increase in Gln with a concurrent slight decrease in Glu (Fig. 3), which would also explain the smaller extent of the α-Glx increase. While this remains to be confirmed by dedicated MRS experiments, possibly at higher fields, it is certain that Glu itself is not increased. A central theorem for hypoxic–ischemic brain damage, however, is the release of the excitatory neurotransmitter Glu from synaptosomes in neurotoxic excess. One explanation for this apparent contradiction is that MRS does not measure local concentrations, i.e., at the synapses, but an average VOI content. Another potential reason for overall reduced Glu tissue content could be leakage of Glu from damaged neurons, particularly as Glu is reported to be of primary neuronal origin (41). We believe it to be probable that Gln synthetase, located in the surviving astrocytes and limited in its capacity by a low ambient Glu concentration (42), acts as a "sink," consuming excess Glu. Therefore, Gln formation might contribute to neuro-protection in hypoxia.

Lac is the end product of glycolytic metabolism of glucose and glycogen and therefore commonly viewed as a marker of anaerobic metabolism, even though many other reasons may lead to an increase in Lac concentration (43). Lac accumulates in acute experimental cerebral hypoxia in animals at the earliest time points (3) and has been regularly observed in MRS studies of stroke (20, 21, 44) and asphyxia (19). In the present context there are a number of interesting observations concerning the accumulation of Lac. First, Lac is singularly absent from the brain spectrum of most patients, even some in whom the outcome was poor. Second, Lac is only modestly elevated on day 1, not reaching its maximum until day 4. Third, when present, excess Lac is a universal marker of poor outcome. The absence of Lac early in the time course is not surprising and provides evidence that virtually all of the intracerebral Lac generated during acute cardiopulmonary arrest can be cleared from the brain within 24 h. It seems likely that later Lac accumulation reflects a secondary effect of brain damage: continued and progressing ischemia as the result of hypoxic damage to the microvasculature or possibly the failure of electron transport and energy metabolism, so that a new intracellular redox equilibrium is established. Since L-Lac is not neurotoxic even at concentrations of 20 mM (45), it is unlikely that the concentrations of 3–5 mM observed in some of the ND patients contribute directly to neurological damage. Two other theories to account for the secondary appearance of Lac should be mentioned. Lac formation by astrocytes, demonstrated in tissue culture, has been proposed as a respiratory substrate for neurons (46). An imbalance between surviving neurons and glial cells might therefore cause an increase in Lac. Also, the Lac production of intruding macrophages has been debated as a source of excess Lac in human stroke (22) and after birth asphyxia (19).

The time course for most spectral abnormalities is similar. The metabolite levels on days 1–2 were mostly still in or near the normal range, and effects developed to maximum extent around days 3–4, with NAA continuing to decrease. The atrophy index α2, which is a measure of the proportion of CSF in the VOI, shows a minimum for the earliest time points indicating that edema, or rather increased intracranial pressure, precedes the maximum metabolic changes. Single investigations, months after ND, show that in severely handicapped patients the metabolic state in the residual brain tissue does not return to normal, i.e., that the metabolite concentrations (particularly NAA) remain far from the norm or that the normal proportion of different cells per volume is not reestablished.

Metabolic disturbances in the two locations chosen for this study appear highly correlated (Fig. 8 *D*). Particularly in bad outcome cases, the deviations from normal are larger for the GM location in parieto-occipital cortex compared with the periventricular WM VOI (data above the diagonal in Fig. 8 *D*). Also, the metabolic disturbances appear to occur somewhat earlier in GM than in WM. However, these expected regional variations reflecting intrinsically differing vulnerabilities or region-dependent inadequate reperfusion are not very large under the present circumstances. The earlier and greater loss of NAA from GM is consistent with the location of the more sensitive neuron cell body here, while progressive loss from WM could be construed as secondary effects on axons.

Prognostic value of MRS in victims of ND. It is tempting to evaluate the MRS findings in terms of their potential for predicting the long-term clinical outcome after ND. At the outset, we caution against drawing firm conclusions regarding patient management because of the small numbers of patients and the severe ethical constraints inherent in such an exercise for which no false results can be tolerated. There is no difficulty in retrospectively segregating good from bad outcome using either NA/Cr or NA or Cr alone or in combination with the elevation of Lac and Glx. At some time point each of these measurements is predictive of outcome. To be of clinical value, prognosis should be defined as early as possible in the postresuscitation period. The combined prognostic index SPI, defined in the above equation and plotted in Fig. 8, is superior to any of the individual metabolites. Already on days 1–2 the good outcome group is clearly separated from the bad outcome group, with some patients, who eventually did badly, still on the borderline to good outcome. 9 of 10 patients with bad eventual outcome were classified correctly within the first 48 h (sensitivity = 90%). On days 3–4 separation between good and bad outcome groups was perfect. One inconclusive result in which early determinations were correct, but apparently refuted by a later MRS result on day 8, must stand as a false negative. More importantly, MRS did not give any false positive results, i.e., prediction of bad outcome in a patient who subsequently did well (specificity = 100%).

Conventional clinical measures applied on day 1 after ND are only 70% accurate in determining outcome, with roughly equal numbers of false positive and false negative predictions. For example, taking GCS after stabilization of 3–4 as predictive of bad outcome, there were three false negative results (sensitivity = 70%) and one false positive (specificity = 75%). ^{1}H-MRS appears to be superior. There was fairly good correlation between GCS and the MRS findings (Kendall τ_b correlation coefficient 0.32 after 48 h and 0.49 for days 3–4), but independent correlation of MRS (τ_b = 0.66 early and 0.68 late) or GCS (τ_b = 0.65) with outcome was higher. Thus, prognosis may improve when using both GCS and ^{1}H-MRS criteria. We anticipate that a clinical trial of a size necessary to establish MRS as an ethically acceptable tool in prognosis after ND or other hypoxic episodes could be undertaken with reasonable chances of success.

This paper confirms and extends the promise of earlier reports of either ^{31}P-MRS or ^{1}H-MRS to identify changes in the brain in human subjects after ischemia, hypoxia, or stroke. It sheds some light on the metabolic repercussions of hypoxia indicating the gradual loss of a neuronal marker and a secondary failure of energy metabolism, possibly reflected by the accumulation of Lac and Gln. By studying ND, in which the hypoxic insult is accurately known and global in nature, much of the uncertainty and variability in MRS findings of other studies has been circumvented. By use of reproducible methods and accurate metabolite quantification, MRS is now shown to be more accurate than clinical methods in defining the severity of hypoxic damage, suggesting an extremely practical clinical role for MRS as an early indicator of ultimate neurological outcome. Perhaps even more important in the long term, is the identification and quantitation of subtle biochemical defects. Through the careful examination of these multiple neurochemical consequences of hypoxic injury, a strategy for prevention and brain salvage may emerge.

Acknowledgments

We thank the Medical Residents and the ICU nurses, as well as Craig Lysy and Respiratory Therapy team (Huntington Memorial Hospital). John Smith of Guardian Ambulance provided emergency transport free of charge. Thanks to J.C. Bellinger for preparing the manuscript.

Support by the Whittier foundation of California, the Altadena Guild, and the Boswell Foundation is gratefully acknowledged.

References

1. Levy, D.E., J.J. Caronna, B.H. Singer, R.H. Lapinski, H. Frydman, and F. Plum. 1985. Predicting outcome from hypoxic-ischemic coma. *J. Am. Med. Assoc.* 253:1420–1426.

2. Edgren, E., U. Hedstrand, S. Kelsey, K. Sutton-Tyrrell, and P. Safar. 1994. Assessment of neurological prognosis in comatose survivors of cardiac arrest. *Lancet.* 343:1055–1059.

3. Duffy, T.E., S.R. Nelson, and O.H. Lowry. 1972. Cerebral carbohydrate metabolism during acute hypoxia and recovery. *J. Neurochem.* 19:959–977.

4. Volpe, J.J. 1987. Neurology of the Newborn. W.B. Saunders Co., Philadelphia.

5. Flynn, C.J., A.A. Farooqui, and L.A. Horrocks. 1989. Ischemia and hypoxia. *In* Basic Neurochemistry: Molecular, Cellular, and Medical Aspects. G.J. Siegel, B.W. Agranoff, R.W. Albers, and P.B. Molinoff, editors. Raven Press, New York. 783–795.

6. Griggs, R.C., and A.I. Arieff. 1992. Hypoxia and the central nervous system. *In* Metabolic Brain Dysfunction in Systemic Disorders. A.I. Arieff and R.C. Griggs, editors. Little, Brown and Company, Boston. 39–54.

7. Ames, A., III, R.L. Wright, M. Kowada, J.M. Thurston, and G. Majno. 1968. Cerebral ischemia. II. The no-reflow phenomenon. *Am. J. Pathol.* 52:437–453.

8. Modell, J.H. 1993. Drowning. *N. Engl. J. Med.* 328:253–256.

9. Witte, M.K. 1990. Near-drowning. *In* Practical Guide to Pediatric Intensive Care. J.L. Blumer, editor. Mosby, St. Louis. 313–317.

10. Orlowski, J.P. 1987. Drowning, near-drowning, ice-water submersions. *Pediatr. Clin. North Am.* 34:75–92.

11. Conn, A.W., J.E. Montes, and G.A. Barker. 1980. Cerebral salvage in near-drowning following neurological classification by triage. *Can. Anaesth. Soc. J.* 27:201–209.

12. Ashwal, S., S. Schneider, L. Tomasi, and J. Thompson. 1990. Prognostic implications of hyperglycemia and reduced cerebral blood flow in childhood near-drowning. *Neurology.* 40:820–823.

13. Bratton, S.L., D.S. Jardine, and J.P. Morray. 1994. Serial neurologic examinations after near-drowning and outcome. *Arch. Pediatr. & Adolesc. Med.* 148:167–170.

14. Connors, R., T.C. Frewen, N. Kissoon, J. Kronick, J. Sommerauer, R. Lee, N. Singh, N. Tiffin, and T. Brown. 1992. Relationship of cross-brain oxygen content difference, cerebral blood flow, and metabolic rate to neurologic outcome after near-drowning. *J. Pediatr.* 121:839–844.

15. Laptook, A.R., R.J.T. Corbett, R. Uauy, C. Mize, D. Mendelsohn, and R.L. Nunnally. 1989. Use of P-31 magnetic resonance spectroscopy to characterize evolving brain damage after perinatal asphyxia. *Neurology.* 39:709–712.

16. Azzopardi, D., J.S. Wyatt, E.B. Cady, D.T. Delpy, J. Baudin, A.L. Stewart, P.L. Hope, P.A. Hamilton, and E.O.R. Reynolds. 1989. Prognosis of newborn infants with hypoxic-ischemic brain injury assessed by phosphorous magnetic resonance spectroscopy. *Pediatr. Res.* 25:445–451.

17. Roth, S.C., D. Azzopardi, A.D. Edwards, J. Baudin, E.B. Cady, J. Townsend, D.T. Delpy, A.L. Stewart, J.S. Wyatt, and E.O.R. Reynolds. 1992. Relation between cerebral oxidative metabolism following birth asphyxia, and neurodevelopmental outcome and brain growth at one year. *Dev. Med. Child Neurol.* 34:285–295.

18. Peden, C.J., F.M. Cowan, D.J. Bryant, J. Sargentoni, I.J. Cox, D.K. Menon, D.G. Gadian, J.D. Bell, and L.M. Dubowitz. 1990. Proton spectroscopy of the brain in infants. *J. Comput. Assisted Tomogr.* 14:886–894.

19. Groenendaal, F., R.H. Veenhoven, J. van der Grond, G.H. Jansen, T.D. Witkamp, and L.S. De Vries. 1994. Cerebral lactate and *N*-acetyl-aspartate/choline ratios in asphyxiated full-term neonates demonstrated in vivo using proton magnetic resonance spectroscopy. *Pediatr. Res.* 35:148–151.

20. Gideon, P., B. Sperling, P. Arlien Soborg, T.S. Olsen, and O. Henriksen. 1994. Long-term follow-up of cerebral infarction patients with proton magnetic resonance spectroscopy. *Stroke.* 25:967–973.

21. Barker, P.B., J.H. Gillard, P.C.M. van Zijl, B.J. Soher, D.F. Hanley, A.M. Agildere, S.M. Oppenheimer, and R.N. Bryan. 1994. Acute stroke: evaluation with serial proton MR spectroscopic imaging. *Radiology.* 192:723–732.

22. Petroff, O.A., G.D. Graham, A.M. Blamire, M. al Rayess, D.L. Rothman, P.B. Fayad, L.M. Brass, R.G. Shulman, and J.W. Prichard. 1992. Spectroscopic imaging of stroke in humans: histopathology correlates of spectral changes. *Neurology.* 42:1349–1354.

23. Ernst, T., R. Kreis, and B.D. Ross. 1993. Absolute quantitation of water and metabolites in the human brain. I. Compartments and water. *J. Magn. Reson. Series B.* 102:1–8.

24. Kreis, R., T. Ernst, and B.D. Ross. 1993. Absolute quantitation of water and metabolites in the human brain. II. Metabolite concentrations. *J. Magn. Reson. Series B.* 102:9–19.

25. Michaelis, T., K.D. Merboldt, H. Bruhn, W. Hänicke, and J. Frahm. 1993. Absolute concentrations of metabolites in the adult human brain in vivo: quantification of localized proton MR spectra. *Radiology.* 187:219–227.

26. Barker, P.B., B.J. Soher, S.J. Blackband, J.C. Chatham, V.P. Mathews, and R.N. Bryan. 1993. Quantitation of proton NMR spectra of the human brain using tissue water as an internal concentration reference. *NMR Biomed.* 6:89–94.

27. Danielsen, E.R., and O. Henriksen. 1994. Absolute quantitative proton NMR spectroscopy based on the amplitude of the local water suppression pulse. Quantification of brain water and metabolites. *NMR Biomed.* 7:311–318.

28. Kreis, R., T. Ernst, and B.D. Ross. 1993. Development of the human brain: in vivo quantification of metabolite and water content with proton magnetic resonance spectroscopy. *Magn. Reson. Med.* 30:424–437.

29. Kreis, R., N. Farrow, and B.D. Ross. 1991. Localized 1H NMR spectroscopy in patients with chronic hepatic encephalopathy. Analysis of changes in cerebral glutamine, choline and inositols. *NMR Biomed.* 4:109–116.

30. Kreis, R., N. Farrow, and B.D. Ross. 1990. Diagnosis of hepatic encephalopathy by proton magnetic resonance spectroscopy. *Lancet.* 336:635–636.

31. Behar, K.L., and T. Ogino. 1993. Characterization of macromolecule resonances in the 1H NMR spectrum of rat brain. *Magn. Reson. Med.* 30:38–44.

32. Jennett, B., and M. Bond. 1975. Assessment of outcome after severe brain damage: a practical scale. *Lancet.* 1:480–484.

33. Adams, J.H., J.A.N. Corsellis, and L.W. Duchen. 1984. Greenfield's Neuropathology. John Wiley & Sons Inc., New York.

34. Birken, D.L., and W.H. Oldendorf. 1989. *N*-acetyl-L-aspartic acid: a literature review of a compound prominent in 1H-NMR spectroscopic studies of brain. *Neurosci. Biobehav. Rev.* 13:23–31.

35. Gill, S.S., R.K. Small, D.G.T. Thomas, P. Patel, R. Porteus, N. VanBruggen, D.G. Gadian, R.A. Kauppinen, and S.R. Williams. 1989. Brain metabolites as 1H NMR markers of neuronal and glial disorders. *NMR Biomed.* 2:196–200.

36. Urenjak, J., S.R. Williams, D.G. Gadian, and M. Noble. 1992. Specific expression of *N*-acetylaspartate in neurons, oligodendrocyte type-2 astrocyte progenitors, and immature oligodendrocytes in vitro. *J. Neurochem.* 59:55–61.

37. Peres, M., D. Bourgeois, S. Roussel, Y. Lefur, P. Devoulon, C. Remy, B. Barrere, M. Decorps, E. Pinard, D. Riche, et al. 1992. Two-dimensional 1H spectroscopic imaging for evaluating the local metabolic response to focal ischemia in the conscious rat. *NMR Biomed.* 5:11–19.

38. Peden, C.J., M.A. Rutherford, J. Sargentoni, I.J. Cox, D.J. Bryant, and L.M.S. Dubowitz. 1993. Proton spectroscopy of the neonatal brain following hypoxic-ischaemic injury. *Dev. Med. Child Neurol.* 35:502–510.

39. Hope, P.L., E.B. Cady, P.S. Tofts, P.A. Hamilton, A.M. del Costello, D.T. Delpy, A. Chu, and E.O.R. Reynolds. 1984. Cerebral energy metabolism studied with phosphorus NMR spectroscopy in normal and birth-asphyxiated infants. *Lancet.* 2:366–370.

40. Lorek, A., Y. Takei, E.B. Cady, J.S. Wyatt, J. Penrice, A.D. Edwards, D. Peebles, M. Wylezinska, H. Owen-Reece, V. Kirkbride, et al. 1994. Delayed ("secondary") cerebral energy failure after acute hypoxia-ischemia in the newborn piglet: continuous 48-hour studies by phosphorus magnetic resonance

spectroscopy. *Pediatr. Res.* 36:699–706.

41. Ottersen, O.P., N. Zhang, and F. Walberg. 1992. Metabolic compartmentation of glutamate and glutamine: morphological evidence obtained by quantitative immunocytochemistry in rat cerebellum. *Neuroscience.* 46:519–534.

42. Kanamori, K., and B.D. Ross. 1995. In vivo activity of glutaminase in the brain of hyperammonemic rat measured by 15N NMR. *Biochem. J.* 305: 329–336.

43. Veech, R.L. 1991. The metabolism of lactate. *NMR Biomed.* 4:53–58.

44. Blamire, A.M., G.D. Graham, D.L. Rothman, and J.W. Prichard. 1994. Proton spectroscopy of human stroke: assessment of transverse relaxation times and partial volume effects in single volume steam MRS. *Magn. Reson. Imaging.* 12:1227–1235.

45. Chan, L., J. Slater, J. Hasbargen, D.N. Herndon, R.L. Veech, and S. Wolf. 1994. Neurocardiac toxicity of racemic D,L-lactate fluids. *Integr. Physiol. Behav. Sci.* 29:383–394.

46. Magistretti, P.J., O. Sorg, N. Yu, J. Martin, and L. Pellerin. 1993. Neurotransmitters regulate energy metabolism in astrocytes: implications for the metabolic trafficking between neural cells. *Dev. Neurosci.* 15:306–312.